JAAS

Accepted Manuscript

This is an *Accepted Manuscript*, which has been through the Royal Society of Chemistry peer review process and has been accepted for publication.

Accepted Manuscripts are published online shortly after acceptance, before technical editing, formatting and proof reading. Using this free service, authors can make their results available to the community, in citable form, before we publish the edited article. We will replace this *Accepted Manuscript* with the edited and formatted *Advance Article* as soon as it is available.

You can find more information about *Accepted Manuscripts* in the Information for Authors.

Please note that technical editing may introduce minor changes to the text and/or graphics, which may alter content. The journal's standard Terms & Conditions and the Ethical guidelines still apply. In no event shall the Royal Society of Chemistry be held responsible for any errors or omissions in this *Accepted Manuscript* or any consequences arising from the use of any information it contains.

ROYAL SOCIETY OF CHEMISTRY

www.rsc.org/jaas

Enhanced method for molybdenum separation and isotopic determination in geological samples and uranium-rich materials

Valérie Migeon[1,2], Bernard Bourdon[1], Eric Pili[2] and Caroline Fitoussi[1]

[1]Laboratoire de Géologie de Lyon (LGL-TPE), ENS Lyon, CNRS and Université Claude Bernard de Lyon, 46 allée d'Italie, 69364 Lyon Cedex 7, France.

[2]CEA, DAM, DIF, F-91297 Arpajon, France.

Table of contents

A three-stage ion exchange chromatography to purified molybdenum from uranium-rich samples was developed. Mo isotopic compositions were analyzed with a Neptune Plus MC-ICP-MS at ~1200 Volt/ppm.

Enhanced method for molybdenum separation and isotopic determination in uranium-rich materials and geological samples

Valérie Migeon[1,2], Bernard Bourdon[1], Eric Pili[2] and Caroline Fitoussi[1]

[1]Laboratoire de Géologie de Lyon (LGL-TPE), ENS Lyon, CNRS and Université Claude Bernard de Lyon, 46 allée d'Italie, 69364 Lyon Cedex 7, France.

[2]CEA, DAM, DIF, F-91297 Arpajon, France.

Abstract

The precise and accurate determination of Mo isotope ratios in geological and U-rich samples requires a thorough separation of Mo from elements that could cause matrix effects and isobaric interferences. These interferences can be attributed to the presence of residual Fe, Ru, Zr and W naturally present in the samples as well as PO_4 contributed by the resin used during chemical separation. Using a three-stage ion-exchange chromatography, we have obtained a high degree of purification with Mo yields ranging between 42 and 80 %. Mo isotopic compositions were measured at a concentration of 30 ng/ml using a Neptune Plus MC-ICP-MS equipped with Jet cones. The sensitivity is ~1200-1600 V/ppm Mo with an aspiration rate of approximately 150 µl per minute. Chemical and instrumental mass dependent fractionations were both corrected using the double-spike method. The total amount of Mo necessary for a single analysis is approximately 45 ng and the typical precision for terrestrial samples is 0.02 ‰ (2 SE, n = 8). This precise and accurate determination of Mo isotope ratios in U-rich samples has the potential for tracing the origin of uranium ores. Another application could be in nuclear forensics, for identifying the separation processes in the nuclear fuel cycle or the provenance of nuclear materials.

1. Introduction

Molybdenum has seven isotopes of masses 92, 94, 95, 96, 97, 98 and 100, with natural abundances ranging from 9.2 to 24.13 %[1]. The isotope composition of Mo can now accurately measured in waters and geological samples, by Multi Collector - Inductively Coupled Plasma - Mass Spectrometry (MC-ICP-MS), with a precision of ~0.1 ‰ (2 SD) using standard bracketing[2], element spiking[3, 4] or double-spike methods[5]. These methods have been used to determine the Mo isotopic compositions in terrestrial samples as well as Mo nucleosynthetic anomalies in meteorites[2, 3, 6-11].

Nuclear forensics was developed for the characterization of nuclear materials in term of chemical or isotope compositions and physical condition interpreted in terms of age, provenance and industrial history. Uranium and molybdenum share a number of common geochemical properties. Under oxidizing conditions, molybdenum and uranium both exist as soluble U(VI) and Mo(VI) species in aqueous solutions while they form insoluble U(IV) and Mo(IV) minerals under reducing conditions. This is also witnessed by their enrichment in anoxic sediments[12-17]. Although Mo is often enriched in uranium ores, the main minerals hosting these two metals (i.e Mo is in molybdenite or pyrite while U is in uraninite) form under slightly different conditions[18]. In uranium ore samples, uranium and molybdenum concentrations vary from a few hundred µg/g to 20 % wt%[19] and a few ng/g to more than 0.5 wt%[20-22] respectively, with U/Mo ratios ranging between 0.1 and 1100[23, 24]. In the nuclear fuel cycle, molybdenum is an impurity that is difficult to separate during uranium enrichment and purification processes[25]. In uranium ore concentrates, uranium grade ranges between 65 and 85 wt% and Mo concentrations must be less than 3 mg/gU[25], leading to U/Mo ratio greater than 280. Uranium purification processes are expected to fractionate Mo isotopes, suggesting that Mo isotopes could be used as a fingerprint in the field of nuclear forensics.

Over the past two decades, a variety of protocols have been developed to separate Mo, principally by ion-exchange chromatography, from interfering elements (i.e. Zr and Ru) and from other matrix elements[5-7, 9, 26]. Malinovsky et al.[4] argued that the Fe/Mo has to be less than 1 to avoid isobaric interferences and that the Si/Mo ratio has to be less than 5 to avoid matrix effects on a Neptune MC-ICP-MS. In this study, we used an enhanced Neptune Plus MC-ICP-MS equipped with Jet cones (sampler Jet cone and X skimmer cone), that improves the sensitivity by a factor of 60, relative to the study of Malinovsky et al.[4]. This higher sensitivity is accompanied with a greater production of isobaric interferences by molecular ions (e.g. $^{56}Fe^{40}Ar^{+}$, $^{55}Mn^{40}Ar^{+}$, $^{64}Zn^{14}N^{16}O^{+}$, $^{58}Ni^{40}Ar^{+}$, $^{40}Ca^{40}Ar^{16}O^{+}$, $^{46}Ti^{40}Ar^{14}N^{+}$) while the matrix effects (U, Si, P, etc.) have to be monitored carefully. Based on existing literature, a target of this study was to develop a Mo separation method such that all majors and interfering elements (X) should have X/Mo<1. This required modifying existing protocols since U-rich matrices have a very different bulk composition compared with silicate rocks or sediments. Some existing protocols are likely to fail for uranium ore concentrates with much higher U/Mo ratios than other samples. Anbar et al.[3], Barling et al.[7] and Pietruszka et al.[2]

used anion and cation exchange resins in HCl media. In these protocols, samples are loaded and rinsed in anion exchange resin in 6M HCl and Mo is eluted with 1M HCl. In 6M HCl media, uranium has a distribution coefficient greater than 10^2 and hence, with our U rich samples, the capacity of this resin would be exceeded. Siebert et al.[5] used an anion-exchange resin with a 2M H_2SO_4 – 0.1% H_2O_2 mixture and 2 M HNO_3 for eluting Mo. According to Strelow and Bothma[27], uranium is probably retained on a resin in this H_2SO_4-H_2O_2 media and may be eluted together with Mo in HNO_3 media. Pearce et al.[9] developed a single-stage separation method on an anion exchange resin. Matrix elements were rinsed with a 1 M HF - 0.5 M HCl mixture (elution of U, Fe, Mn, Ni) and 4 M HCl (elution of Zr and Pb) before the elution of Mo in 3 M HNO_3. Separation of Mo has also been studied with chelating resin[4] and using solvent extraction[28, 29]. In contrast, Burkhardt et al.[6] used five columns to obtain a high degree of Mo purification. First, a cation exchange resin allowed the separation of Mo (along with Ti, W, HFSE and Ru) from major elements in 1 M HCl- 0.1 M HF. Second, an anion resin was used to elute Fe, Ni and Ru with 1 M HF, then Ti, Zr, Hf and W with a mixture of HCl-HF while Mo was collected with 3 M HNO_3. Finally, the specific cationic TRU-Spec resin was used three times to isolate Mo from Ru traces. More recently, Le Boudec et al.[26] developed an anion exchange procedure allowing the separation of Mo from major elements including U, with a mixture of 0.6 M HCl and 0.01 % H_2O_2, Ruthenium and traces of Fe were then eluted with 0.05 M HNO_3- 0.03 M HF, while Mo was eluted using 4 M HNO_3-0.03 M HF. It has been shown that ion-exchange chromatography could induce mass dependent fractionation of Mo isotopes due to a loss of Mo during chemical separation[3, 5]. Thus, mass dependent fractionation induced by chemical separation must be corrected with the addition of a double spike (see section below).

In this study, we have developed a new ion-exchange procedure to separate molybdenum from its interfering elements in a uranium-rich matrix. We used geological and uranium ore concentrate standard materials to test and improve the robustness of our method for various types of matrices. A combination of two anion and one cation exchange resins were used to reduce the U/Mo ratio to $<2x10^{-4}$, as well as Zr/Mo$<5x10^{-3}$, Ru/Mo$<6x10^{-4}$ for all samples, with yields ranging from 42 to 80 %. The double-spike technique, using a ^{97}Mo-^{100}Mo mixture was used to correct for chemical and instrumental mass-dependent isotope fractionation. This mass spectrometric analysis yielded a precision of 0.05 to 0.12 ‰ (2 SD), for Mo standard solutions and samples, which is similar to recently published methods.

2. Experimental methods

2.1. Materials, reagents and sample digestion

All reagents were distilled, once for HNO_3 and HCl, twice for HF, with Savillex® PFA stills. Ultrapure water was produced with a Millipore Integral 10 deionization system. Samples and synthetic solutions were prepared in PFA Savillex® beakers. They were cleaned

by refluxing at ~130°C with 50 % HNO_3, 50 % HCl and mixtures of concentrated HNO_3-HF and HCl-HF. They were finally rinsed with ultrapure water.

First, the purification protocol of molybdenum was developed with synthetic solutions. These solutions were prepared by mixing and diluting plasma standard solutions of Mo, Zr, Ru, W, Fe and U from the Johnson Matthey Company (Alpha Aesar Specpure®). Three types of solid samples were used to test and improve the purification (Table 1). Geological standards include magmatic rocks (three basalts: BHVO-2, BE-N and BR, one andesite: AGV-1) and a sedimentary rock (a bauxite: BX-N). The latter sample was chosen because of its distinct Al-rich matrix with iron-oxides and a high Mo content. Uranium reference materials are uranium ore concentrates distributed by CETAMA [24] (France): Bolet and Chanterelle are U_3O_8, produced by calcination of ammonium diuranate and doped with unknown multi-element solutions, including Mo. Grenat and Calcedoine are a sodium diuranate ($Na_2U_2O_7.6H_2O$) and a magnesium diuranate ($MgU_2O_{7.}6H_20$), respectively. Their compositional variations are due to different methods of uranium precipitation.

Before ion-exchange chromatography, the solid samples were ground and then digested in acid mixtures. Between 100 and 400 mg of geological standard were dissolved using 6 ml of concentrated HNO_3-HF 1:1 mixture at 120 °C in Savillex® beakers over at least 48 hours. Perchloric acid was added to this mixture before evaporation (one drop per ml of HF). Samples were then evaporated to dryness at 160 °C. Deionized water was added several times and the solution was dried to eliminate traces of perchloric acid. Then, the samples were redissolved several times with ~ 5 ml of hot concentrated HCl to remove remaining fluoride traces. Uranium reference material powders were digested with a mixture of 8 M HNO_3 and 0.1 M HF at 100 °C in Savillex® beakers over 48 h.

Mo purification was done using two anion exchange resins AG1-X8, 100-200 mesh in Cl-form (Biorad, analytical grade) and an actinide specific TRU Spec resin, 100-150 µm (Eichrom). Two Mo standard solutions were used to test the chemical separation. The NIST-SRM 3134 solution was chosen as the Mo reference standard for isotopic measurements, following Wen et al.[30], Greber et al.[31] and Goldberg et al.[32]. The secondary standard (hereafter ENS-Lyon Mo) was an Alfa Aesar plasma standard solution.

Table 1: Mo data for samples and standards

Sample	Material[1]	U/Mo $_{initial}$[1]	U/Mo $_{final}$	Digestions[2]	Mo (µg/g)[3] ± 2 SD	Mo (µg/g)[4] ± 2 SD	δ^{98}Mo (‰) ± 2 SE	Analyses
Uranium ore concentrates								
Bolet	U_3O_8	2.05×10^{5}	1.97×10^{-5}	2	4.18 *± 0.01*	*4.14 ± 0.42*	-0.33 ± 0.02	8
Chanterelle	U_3O_8	1.85×10^{4}	1.79×10^{-5}	2	44.8 ± 3.0	*45.8 ± 3.4*	0.05 ± 0.02	9
Grenat	$Na_2U_2O_7.6H_2O$	1.48×10^{3}	1.89×10^{-5}	2	455.2 ± 25.8	*419.0 ± 20.3*	-2.84 ± 0.03	9
Calcedoine	$MgU_2O_{7.}6H_2O$	5.07×10^{2}	1.80×10^{-5}	2	1371.97 ± 70.94	*1189.4 ± 70.0*	-1.82 ± 0.03	4
Geological standards								
BHVO-2	Basalt	0.10	1.80×10^{-5}	3	4.4 ± 1.0	*3.9 ± 2.3*	-0.04 ± 0.02	7
BE-N	Basalt	0.86	1.92×10^{-5}	2	2.38 ± 0.03	*2.8 ± 0.3*	-0.39 ± 0.02	8
BR	Basalt	1.04	2.76×10^{-5}	1	2.1 *± 0.3*	*2.2 ± 0.2*	-0.57 ± 0.03	4
AGV-1	Andesite	0.90	3.29×10^{-5}	1	1.8 ± 0.3	*2.3 ± 0.2*	-0.18 ± 0.05	6
BX-N	Bauxite	1.20	1.82×10^{-4}	1	7.58 *± 0.01*	*8.3 ± 0.5*	0.29 ± 0.02	8

[1] Nature and U/Mo $_{initial}$ are obtained from CETAMA[24] for the uranium ore concentrates and from GeoReM for the geological standards; [2] Number of digestion replicates for each sample; [3]Mo concentrations, measured by isotope dilution; [4] Published Mo concentrations for the uranium ore concentrates[24], BHVO-2[33], BE-N and AGV-1[34], BR[35] and BX-N[36]. 2 SD and 2 SE corresponds to the standard deviation and the standard error of the mean, respectively.

2.2. Double spike

Isotope compositions measurements by MC-ICP-MS require an instrumental mass bias correction to obtain the natural isotopic compositions of samples. A variety of measurement protocols have been developed: standard bracketing[2], element spiking[3, 4] or double-spike (DS) methods[5]. The main advantage of the DS method is to correct both the instrumental mass bias and mass-dependent fractionation that takes place during chemical separation[5, 37-39]. Thus, the DS method does not require a quantitative recovery of Mo. ^{97}Mo and ^{100}Mo isotopes were chosen as double spike because of the low error magnification during the double-spike inversion[40], their availability at a high purity, and because these masses are relatively free of isobaric interferences. Only ^{100}Mo has a small interference from ^{100}Ru that can be corrected for (see section 3.4). According to the work of Rudge et al.[40] to minimize the error estimation in the natural fractionation of a sample, spikes of ^{97}Mo and ^{100}Mo were mixed in proportion of 42.57 wt% and 57.43 wt% respectively. They were purchased from Oak Ridge National Laboratory, with a purity of 94.2 % for ^{97}Mo and 97.2 % for ^{100}Mo, with traces of other Mo isotopes. Prior to Mo purification, Mo concentrations in samples were first measured by isotope dilution with a Thermo Neptune Plus or a Nu 500 MC-ICP-MS. An aliquot of each sample containing ~400 ng of Mo was then mixed with ~556 ng Mo of double spike solution, targeting the following sample-spike proportions[40]: 58.18 wt% of the total Mo coming from the DS and 41.82 wt% from the sample.

2.3. Ion-exchange chromatography

Molybdenum purification from sample matrix was performed using a three-stage ion-exchange chromatography (Table 2). After double spike addition, samples were homogenized with a mixture of concentrated HCl-H_2O_2 to destroy any organic matter (1 ml of each reagent). They were then evaporated to near-dryness at 120°C, and dissolved in 1 ml of 1 M HCl + 0.02 % H_2O_2 before being loaded on an anion exchange resin (2 ml of AG1-X8, 100-200 mesh). Prior to loading, the anion resin column was washed with 0.5 M HNO_3, 0.2 M HCl and 5 M HNO_3 + 0.03 M HF and the column was conditioned with 1 M HCl + 0.02 % H_2O_2. Uranium and matrix elements were washed with 0.6 M HCl + 0.02 % H_2O_2 and 0.05 M HNO_3 + 0.03 M HF. The addition of hydrogen peroxide to the HCl solution increased significantly the distribution coefficient of Mo[41]. Ruthenium traces and tungsten, which create isobaric interferences with Mo isotopes, were eluted with 1 M HF and 6 M HCl + 1 M HF, respectively[6]. Mo was then collected with a 5 M HNO_3 + 0.03 M HF mixture. The presence of hydrofluoric acid which reduces the partition coefficient of Mo increases the Mo recovery[26, 42], and reduces the elution volume of Mo. Further separation of Mo from remaining elements was achieved with a 1 ml TRU-Spec resin column. Ru and W were eluted with 8 M HNO_3, Fe and Zr with 1 M HCl, while U traces were fixed on the resin. Mo was then collected with 0.1 M HNO_3. At this stage, the Mo fraction was contaminated by phosphate released from the TRU Spec resin. To remove the phosphate that causes isobaric interferences and/or matrix effects during mass spectrometric measurements, the samples were dissolved in 1 M HCl + 0.02 % H_2O_2 and loaded on the same AG1-X8 anion exchange resin column, previously pre-cleaned. Phosphate was washed off the resin using 0.6 M HCl + 0.02 % H_2O_2 and Mo was collected with 5 M HNO_3 + 0.03 M HF.

Concentrations of Mo and other elements, at different steps of the column calibrations were checked with an Agilent 7500 and a Thermo Element II ICP-MS at ENS Lyon to check the purity of the final Mo elution and reagents.

Table 2: Mo purification scheme

Step	Reagent	Volume (ml)
1. Anion exchange resin (AG1-X8, 100-200 mesh, 2 ml)		
Conditioning	HCl 1N + H_2O_2 0.02%	8
Load	HCl 1N + H_2O_2 0.02%	1
Wash matrix	HCl 0.6N + H_2O_2 0.02%	40
Wash Ru + Fe traces	HNO_3 0.05N + HF 0.03N	25
Wash Ru traces	HF 1N	25
Wash W	HCl 6N + HF 1N	12
Collect Mo	HNO_3 5N + HF 0.03N	14
2. Cation exchange resin (TRU Spec resin, 100-150 µm, 1 ml)		
Conditioning	HNO_3 8M	5
Load	HNO_3 8M	1
Wash Ru, W	HNO_3 8M	4
Wash Zr, Fe	HCl 1M	6
Collect Mo	HNO_3 0.1M	5
3. Anion exchange resin (AG1-X8, 100-200 mesh, 2 ml)		
Conditioning	HCl 1N + H_2O_2 0.02%	8
Load	HCl 1N + H_2O_2 0.02%	1
Wash P	HCl 0.6N + H_2O_2 0.02%	40
Collect Mo	HNO_3 5N + HF 0.03N	14

3. Mass spectrometry

3.1. MC-ICP-MS measurements

Mo isotope measurements were performed in a low resolution (400) mode using static multi-collection with a Thermo Neptune Plus MC-ICP-MS at ENS Lyon. The maximum spacing of the nine Faraday cups corresponds to a total mass dispersion of ~9 amu in the Mo mass range: ion beam intensities of all seven molybdenum isotopes plus ^{91}Zr and ^{99}Ru were thus measured simultaneously (Table 3). Ru and Zr isobaric interferences were monitored to allow corrections, if necessary. A sampler Jet cone, associated with an X-skimmer cone, were used to improve the sensitivity by a factor close to 10, compared to normal-type cones used by Li et al.[33] with a Neptune Plus. However, at the optimum sensitivity, the formation of polyatomic ions was observed in 0.05 M HNO_3 blank solutions in the Mo mass range. They correspond to molecules containing Ar and N which are very abundant in the plasma. To reduce these isobaric interferences below 10 mV, argon, nitrogen and sample gas flow of the desolvating unit (Aridus II) were adjusted, while maintaining a good stability of the signal. Under these conditions, we observed that the ENS-Lyon Mo and the NIST-SRM 3134 standards data followed the expected mass fractionation for all isotope ratios, except for isotope ratios involving ^{94}Mo. This means that, overall, the level of isobaric interferences formed in the plasma on the Mo mass spectrum was sufficiently low, except at 94 amu.

Table 3: Cup configuration on the Neptune Plus for the Mo isotope analysis, with Mo, Zr and Ru abundances.

Cup configuration									
Cup	**L4**	**L3**	**L2**	**L1**	**C**	**H1**	**H2**	**H3**	**H4**
Mass	91	92	94	95	96	97	98	99	100
Abundances (%)									
Molybdenum		14.84	9.25	15.92	16.68	9.55	24.13		9.63
Zirconium	11.22	17.15	17.38		2.80				
Ruthenium							1.88	12.70	12.60

3.2. Double-spike calibration

The DS data inversion requires four isotopes. We chose the following isotopes ^{95}Mo, ^{97}Mo, ^{98}Mo and ^{100}Mo, while ^{95}Mo was used as the normalizing isotope since it was relatively free of isobaric interferences. The double spike was first calibrated using mixtures of the standard NIST-SRM-3134 solution with the ^{97}Mo-^{100}Mo spike. The following equations were used to determine the composition of the spike (T_i):

$$n_i = n_i' e^{\alpha_0 P_i} \quad (1)$$

$$m_i = M_i e^{\beta P_i} \quad (2)$$

$$M_i = \lambda T_i + (1-\lambda) N_i \quad (3)$$

$$m_i e^{-\beta P_i} = \lambda T_i + (1-\lambda) n_i' e^{-\alpha_0 P_i} \quad (4)$$

where n_i is the true isotopic ratio composition of the standard NIST-SRM-3134 (e.g. ^{98}Mo/^{95}Mo), whereas n'_i corresponds to the measured ratio of this standard. P_i is the natural log of the atomic masses (e.g. 97.9054073/94.9058411). M_i and m_i represent the true and measured ratios of the spike-standard mixture respectively, and T_i are the true ratios of the DS. α_0 and β are the unknown instrumental mass dependent fractionation factors for the standard and spike-standard mixtures, respectively. The first two equations assume that isotope ratios are fractionated following the exponential law. λ is the proportion of DS in the mixture. Multiplying equation (4) by $e^{\alpha_0 P_i}$, one obtains:

$$m_i e^{-\beta' P_i} = \lambda T_i' + (1-\lambda) n_i' \quad (5)$$

where

$\beta' = \beta - \alpha_0$ and $T_i' = T_i\, e^{\alpha_0 P_i}$.

The ^{97}Mo-^{100}Mo double spike was calibrated to obtain values of T_i', which represent calibrated values of the spike isotope ratios relative to the measured value of the NIST standard. T_i' was determined using three spike-standard mixtures in proportion 1:2, 1:1 and 2:1. From these three mixtures, nine equations can be written with nine unknowns (3 values

for λ, 3 values for T_i' corresponding to three isotope ratios and 3 values for β' corresponding to the three standard-DS mixtures), which permits to obtain λ, T_i' and β' for each spike-standard mixture. All standards and standard-spike mixtures were measured during the same session. The equations were solved using a Levenberg-Marquardt iteration scheme for the system of non-linear equations (5). True values (T_i) obtained for the double spike are: $^{97}Mo/^{95}Mo$ = 113.6955 ± 0.0013, $^{98}Mo/^{95}Mo$ = 5.6430 ± 0.0009 and $^{100}Mo/^{95}Mo$ = 160.4831 ± 0.0009. Errors are given as 2 SD.

3.3. Data analysis method

Prior to sample analysis, a sequence with two interspersed Mo standards (NIST-SRM-3134 and ENS-Lyon Mo) was launched to check the stability of the instrumental mass-dependent fractionation. Then, samples were bracketed by two analyses of a NIST-SRM-3134 standard solution mixed with the double spike in proportions similar to those of the samples. Sample and standard solutions were introduced as 0.05 M HNO_3 solutions with an uptake rate of ~150 µl/min with a CETAC Aridus II desolvating system using an $Ar+N_2$ mixture. Mo solutions were measured at 30 ng/ml (~ 45 ng of Mo per analysis), allowing a good reproducibility and no Faraday cup saturation (<50 V). Ion beam intensities were around 8 V on ^{95}Mo and higher for the two spiked isotopes: around 30 V on ^{97}Mo and around 40 V on ^{100}Mo. The sensitivity was ~1200 to 1600 V/ppm. Pearce et al. [9], with a Nu Instrument MC-ICP-MS for an uptake rate of 80 µl/min and a Mo concentration of 100 ng/ml, obtained a signal ten times lower than what is reported here. Before sample introduction, the system was cleaned over 300 s with 0.5 M HNO_3 including traces of HF, and then with 0.05 M HNO_3 over 200 s.

Each measurement consisted of 40 cycles with an integration time of 8 seconds per cycle. The Mo peak was centered at the beginning of each run. Effects of low level isobaric interferences were removed using on-peak zeroes, corresponding to the average signal of twenty cycles measured in the blank solution (0.05 M HNO_3) before and after each sample.

Ion beam intensities of Mo isotopes, ^{91}Zr and ^{99}Ru were measured at each cycle. Outliers were filtered on-line with a two-sigma rejection test and less than 5 % of the data points were rejected over 40 cycles per analysis.

3.4. Data reduction

This section describes the various steps used to determine the natural Mo isotope fractionation relative to the NIST-SRM 3134 standard. First, the averaged signal measured in HNO_3 0.05 M blanks, before and after each samples, is subtracted. It corresponds to the level of molecular interferences produced in the plasma (e.g. Ar_2N^+ or Ar_2O^+).

The second step, if necessary, is the correction of isobaric interferences. Ion beam intensities for ^{91}Zr and ^{99}Ru measured in samples were less than 10 mV and 0.1 mV,

respectively. Mo intensities were thus corrected for Zr interferences at masses 92, 94 and 96, and for Ru interferences at masses 96, 98 and 100. The first step was to determine the instrumental fractionation factor f_{Mo} using the exponential law (equation 6-7). f_{Mo} was calculated from average values of unspiked standard solution at the beginning of each session. We chose ^{95}Mo and ^{97}Mo for the determination of f_{Mo} because theses masses are free of Zr and Ru interferences.

$$\left(\frac{^{97}Mo}{^{95}Mo}\right)_{meas} = \left(\frac{^{97}Mo}{^{95}Mo}\right)_{nat} \text{ x } \left(\frac{97}{95}\right)^{f_{Mo}} \quad (6)$$

where $(^{97}Mo/^{95}Mo)_{meas}$ is the measured ratio and $(^{97}Mo/^{95}Mo)_{nat}$ is the natural abundance ratio used for determining fMo.

$$f_{Mo} = \frac{ln\left(\left(\frac{^{97}Mo}{^{95}Mo}\right)_{meas} / \left(\frac{^{97}Mo}{^{95}Mo}\right)_{nat}\right)}{ln\left(\frac{97}{95}\right)} \quad (7)$$

The interference correction was applied, written here for the ^{98}Mo/^{95}Mo ratio:

$$\left(\frac{^{98}Mo}{^{95}Mo}\right)_{corr} = \left(\frac{^{98}T}{^{95}Mo}\right)_{meas} - \left(\left(\frac{^{99}Ru}{^{95}Mo}\right)_{meas} \text{ x } \left(\frac{^{98}Ru}{^{99}Ru}\right)_{nat} \text{ x } \left(\frac{98}{99}\right)^{f_{Mo}}\right) \quad (8)$$

where $(^{98}Ru/^{99}Ru)_{nat}$ is the natural abundance ratio. The corrected Mo isotope ratio $(^{98}Mo/^{95}Mo)_{corr}$ is calculated by removing from the total signal at mass 98 (^{98}T) the contribution of the interfering masses calculated with the relative abundance of another isotope and using the instrumental fractionation factor determined for Mo isotopes. In the example given in equation (8) for mass 98, the respective abundances of Mo and Ru are 24.13 and 1.88 %, respectively. We assumed here that $f_{Ru} = f_{Mo}$, while the ^{98}Ru/^{99}Ru ratio used in equation (8) corresponds to the natural abundance of Ru.

Rudge et al.[40] developed a Matlab® program for calculating the chemical and instrumental mass fractionation corrections, using the exponential fractionation law. First, using the measured Mo isotope ratios in the mixture, the natural fractionation of the sample relative to the standard (α) was calculated with standard mixing equations. Second, the Mo isotope data obtained for samples were expressed as δ^{i}Mo, which is the deviation, in per mil, relative to the NIST standard solution. Double spiked NIST-SRM 3134 solutions were measured before and after every sample. The inversion of the DS NIST-SRM 3134 standards should in principle result in δ^{i}Mo=0 ‰. However, as observed by Burkhardt et al.[43], this is not the case, owing to small deviations in instrumental mass-dependent fractionation from the exponential fractionation law. Therefore, the δ^{i}Mo values of the samples were further corrected using the sample-standard bracketing method using the following equation:

$$\delta^{i/95}Mo_{corr} \approx \delta^{i/95}Mo_{meas} - \delta^{i/95}Mo_{NIST-SRM-3134\,(n-1\,;\,n+1)} \quad (9)$$

Using this procedure, the external reproducibility of samples and standard solutions treated as samples improved significantly (see results below).

4. Chemical separation of Mo from a U-rich matrix

A good purification of Mo required the separation from the sample matrix and from elements that can cause elemental or molecular isobaric interferences. As mentioned above, the chemical separation was first tested with synthetic solutions with enhanced levels of potentially interfering elements. Elution curves are reported in Figure 1. In this study, the main matrix elements are U for uranium-rich samples, and Fe, Al, Ca and Mg for other geological samples. For example, in addition to matrix effects[4], Fe can produce $ArFe^+$ molecules that interfere with Mo isotopes at 94, 96 and 97 amu. In our measurement conditions, the Fe/Mo ratio had to be less than 0.1 to avoid any measurable interference on masses used in the double spike inversion (95, 97, 98 and 100).

Matrix elements were principally separated on the anionic resin column with a Mo yield >90 % for synthetic solution and samples. Recovery is calculated as the ratio between the total amount of Mo in the sample solution prior to chemistry and the total amount of Mo in the final purified solution. The TRU-Spec column was then used to eliminate the remaining traces of matrix elements (principally U), with a recovery close to 77 % for the synthetic solution. The Mo fraction was further purified from phosphate released by degradation of the TRU-Spec resin on a second anion exchange resin column. Overall yields were between 59-76 % for uranium ore concentrates and between 48-82 % for geological standards. For samples containing ~300 ng Mo or less, the resulting purification was generally achieved with $U/Mo<2x10^{-4}$, $Zn/Mo<0.3$, $Zr/Mo<5x10^{-3}$, $Ru/Mo<6x10^{-4}$, $W/Mo<3x10^{-3}$, $Fe/Mo<4x10^{-3}$ and $P/Mo<0.2$ (Table 1). This separation method was specifically designed for uranium-rich matrix, with an elimination of uranium close to 100 %. Traces of iron and zirconium were probably derived from the 5 M nitric acid used for the Mo elution, and ruthenium was generally below the detection limit. The procedural blank was between 0.2 and 1 ng Mo, corresponding to < 0.25 % of the sample Mo, with no effects on the measured Mo isotopic composition of the samples.

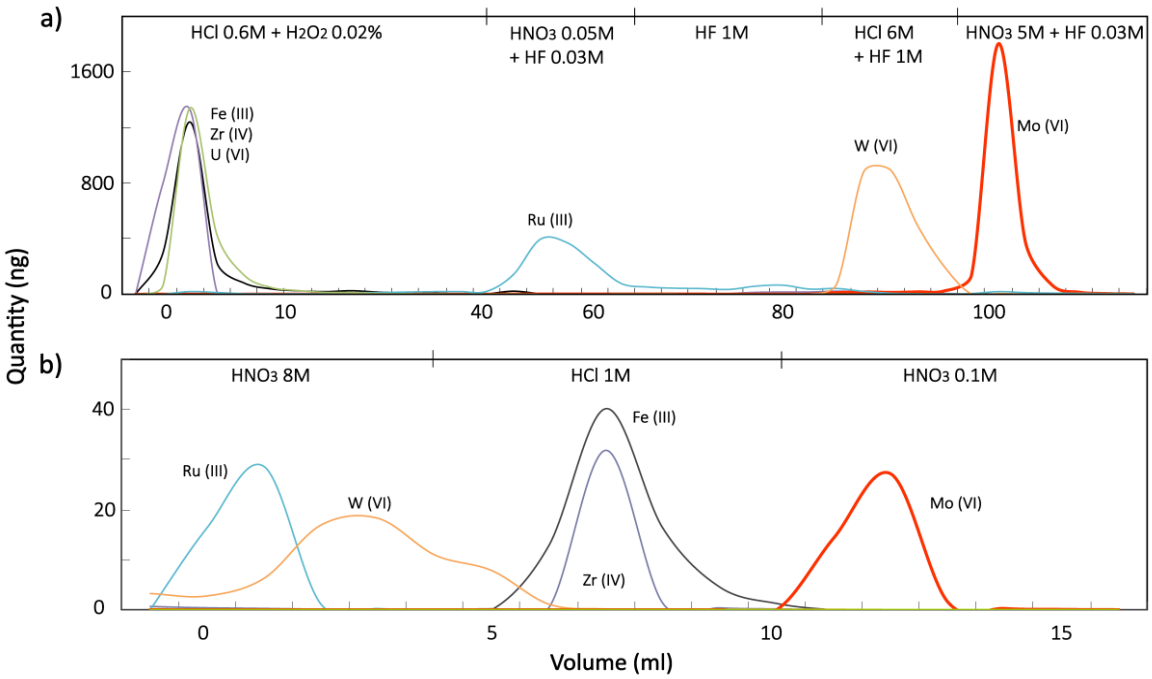

Figure 1: Elution curves of Mo, U, Fe, Zr, Ru and W for (a) the anionic resin AG1-X8, 100-200 mesh and (b) the cationic TRU-Spec resin. Calibration was done for (a) 2 µg and (b) 50 ng of each element and is similar for geological and uranium-rich materials. Details are given in the text.

As a test, the entire Mo separation procedure was done with a NIST-SRM-3134 standard and the BHVO-2 basalts with no double spike. The analysis by standard bracketing yielded δ^{98}Mo of -1.15 ± 0.03 ‰ (2 SE, n = 5) for the NIST-SRM 3134 and -1.87± 0.03 ‰ (2 SD) for BHVO-2, indicating mass dependent Mo isotope fractionation during ion chromatographic separation. Using the same procedure with a ^{97}Mo-^{100}Mo double spike, the δ^{98}Mo value was -0.02 ± 0.03 ‰ (2 SE, n =14) for the NIST-SRM 3134 and -0.04 ± 0.02 ‰ (2 SE, n = 7) for BHVO-2, for a yield close to 66 %. This result shows that the addition of the double-spike efficiently corrected for chemical and instrumental fractionations, even without a 100 % yield.

5. Standard reproducibility

The spiked NIST-SRM-3134 standard solution was measured several times during each analytical session to control the stability of the signal and between each sample. The average results of δ^{98}Mo for nine measurement sessions are shown in Figure 2. Results for individual sessions gave δ^{98}Mo values between 0.016 and 0.136 ‰ while the overall reproducibility is 0.02 ‰ (2 SD), for a sensitivity of ~1200-1600 V/ppm (aspiration rate ~ 150 µl/mn). This precision is better than those previously reported in literature, which ranges from 0.06 to 0.20 ‰ for a sensitivity of 2 to 200 V/ppm[2-9, 31, 33, 44, 45]. Our higher sensitivity, combined with a complete separation of elements producing interferences and with a careful monitoring of isobaric interferences, probably explains the better performance obtained in this study and

allows to measure very low Mo amounts of 45 ng or less. All previous studies required a Mo quantity ranging between 0.1 to 10 µg, except for the work of Duan et al.[8] that used 25 ng per run.

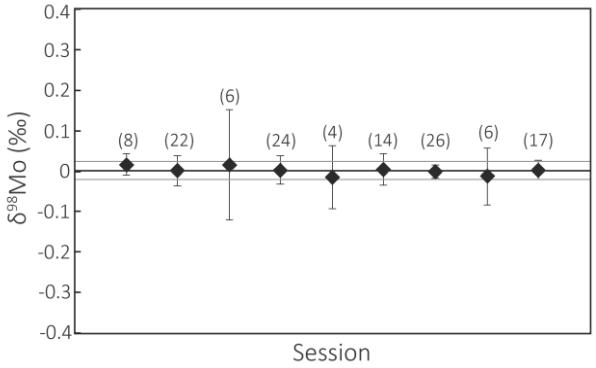

Figure 2: Reproducibility of the δ^{98}Mo measurements for the double-spiked NIST-SRM-3134 solution for nine sessions. Each point corresponds to the average of a number of measurements (given in brackets) during one session. Errors bars represent the two-standard errors (2 SE) of the mean. The mean of the long-term reproducibility is shown by the black line at 0.001 ‰ with a long-term precision of 0.02 ‰ (2 SD, dashed lines).

The instrumental mass-dependent isotope fractionation was checked by measuring the two interspersed Mo standards (NIST-SRM-3134 and ENS-Lyon Mo) without double spike. The slope given by plotting the δ^{98}Mo versus δ^{97}Mo yielded a value of 1.449 ± 0.170, indistinguishable from the theoretical slope of 1.5. All results plot on the mass-fractionation line, indicating no isobaric interferences for the isotopes considered (^{95}Mo, ^{98}Mo and ^{97}Mo).

The δ^{98}Mo (± 2 SD) for the ENS-Lyon Mo standard and each sample, relative to the NIST-SRM-3134 solution, are reported in Figure 3. The ENS-Lyon Mo standard has a δ^{98}Mo of -0.25 ± 0.02 ‰, similar to the Bern-Mo ICP-MS standard solution, with a δ^{98}Mo of -0.27 ± 0.06 (2 SD)[32]. Both solutions were purchased from the Johnson Matthey Company.

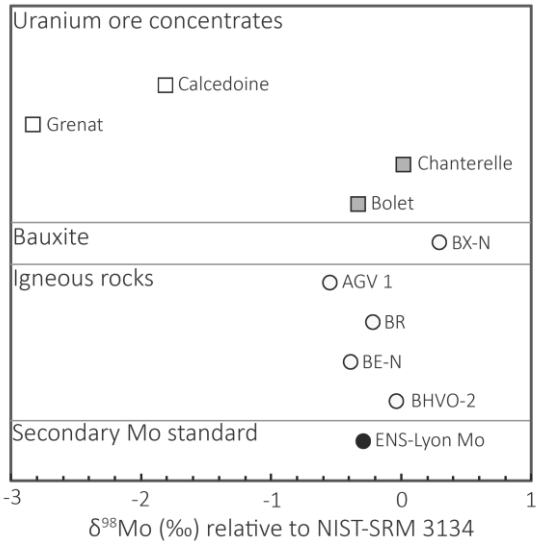

Figure 3: δ^{98}Mo (the error (2 SE) is smaller than the symbol size) relative to the NIST-SRM-3134 for the ENS-Lyon Mo standard solution, geological standards (igneous rocks, bauxite) and uranium reference materials (uranium ore concentrates): U_3O_8 (open square), magnesium- and sodium-diuranate (grey square).

6. Application to geological and uranium-rich samples

All cited literature data were recalculated using the calibration of Goldberg et al.[32], relative to the NIST-SRM 3134 molybdenum standard, for comparison with our results. All igneous rocks analyzed here have Mo concentrations ranging between 1.8 and 4.4 µg/g, which is consistent with the reported range from 0.7 to 19.1 µg/g[46]. Similarly, their δ^{98}Mo values range between -0.57 and -0.04 ‰, which is in agreement with the range reported in the literature for igneous rocks[46] (-0.36 to -0.02 ‰). BHVO-2 gave an average Mo concentration of 4.4 ± 1.0 µg/g (2 SD). This result was obtained by isotopic dilution for three independent digestions (Table 1) and agrees with literature values[9, 47]. In this study, BHVO-2 yielded a δ^{98}Mo value of -0.04 ± 0.02 ‰ (2 SE, n = 7). This is consistent with the data reported in Burkhardt et al.[43] and Li et al.[33], -0.06 ± 0.03 ‰ (2 SE, n = 23) and -0.05 ± 0.06 ‰ (2 SE, n = 3), respectively, but different from the value of Pearce et al.[9] (-0.29 ± 0.04 ‰, 2SE, n = 6). Our data were measured for different digestions and measurement sessions for each sample, whereas Pearce et al.[9] reported measurements for a single measurement session. Furthermore, it is suspected that their separation scheme did not yield the high degree of purity obtained here and by the two other above-cited studies[33, 47]. We reproduced the molybdenum separation scheme described by Pearce et al.[9] to investigate the difference in δ^{98}Mo value obtained for BHVO-2. Following this procedure, two separate digestions of 200 mg were done, one being spiked with our ^{97}Mo-^{100}Mo double spike. The Mo yield was close to 62 %. Mo isotope ratios were measured with our collector configuration (Table 4) and data were corrected from Zr and Ru isobaric interferences. The spiked BHVO-2 yielded a

δ^{98}Mo value of -0.14 ± 0.04 (2 SE, n = 3) which approaches the value reported in Pearce et al.[9] (see discussion below). ε^{i}Mo values were calculated from the unspiked BHVO-2 using ^{98}Mo/^{95}Mo = 1.535 as the normalization ratio used in the mass fractionation correction to identify matrix and/or spectral interferences.

$$\varepsilon^{i/95}Mo = \left[\frac{{}^{i}Mo/{}_{95}Mo \;\; sample,mdf\ corr}{{}^{i}Mo/{}_{95}Mo \;\; NIST-SRM\ 3134\ (n-1;n+1),mdf\ corr} - 1 \right] \times 10^{4} \qquad (10)$$

ε^{i}Mo values for the unspiked BHVO-2 separated using the procedure of Pearce et al.[9] were significantly higher than those obtained with our separation procedure, and δ^{i}Mo/amu were not constant, suggesting that some interferences were not corrected and possibly explaining the lower δ^{98}Mo value for double-spike corrected analysis. Potentially interfering elements found in the final Mo cut were Zn, Ti, Ca and Fe, with Zn/Mo ~ 33, Ti/Mo ~ 1.4, Ca/Mo ~ 1.3 and Fe/Mo ~ 0.7.

Table 4: Mo fractionation in BHVO-2 basalt sample.

BHVO-2 basalt	δ^{98}Mo ± 2 SD[1]	Mass	92[2]	94[2]	96[2]	97[2]	98[2]	100[2]
BHVO-2, this study	-0.04 ± 0.02	ε^{i}Mo	1.88	0.67	0.44	1.77	0.00	2.40
		δ^{i}Mo/amu	-0.71	-0.71	-0.59	-0.54	-0.62	-0.57
BHVO-2, with Pearce et al.[9] separation	-0.14 ± 0.06	ε^{i}Mo	7.95	7.18	20.55	0.32	0.00	9.72
		δ^{i}Mo/amu	-0.60	-1.05	1.73	-0.31	-0.32	-0.12

[1] δ^{98}Mo obtained for spiked-BHVO-2 after the double-spike inversion; [2] Values obtained for unspiked BHVO-2 in ε^{i}Mo and δ^{i}Mo/amu.

BX-N, a bauxite sample derived from a weathered limestone, gave a Mo concentration of 7.58 ± 0.01 µg/g (2 SD) and a δ^{98}Mo value of 0.29 ± 0.02 ‰ (2 SE, n = 8) which is consistent with the range reported for carbonate rocks[48] (-0.17 to 1.93 ‰). Voegelin et al.[48] suggested that these variations in Mo isotope signatures could be explained by Mo derived from skeletal components, input of detrital materials, or addition of light Mo isotopes brought by hydroxides via diagenetic fluids. The effect of bauxitization on Mo isotopes is in itself unknown.

Four uranium-rich standards, from CETAMA[24], were used to test the Mo separation. The two uranium oxides (U_3O_8), Bolet and Chanterelle, have a Mo concentration of 4.18 ± 0.01 µg/g and 44.8 ± 3.0 µg/g (2 SE), and δ^{98}Mo of -0.33 ± 0.02 ‰ and 0.05 ± 0.02 ‰ (2 SE), respectively. The two diuranate samples, Grenat and Calcedoine, show a higher Mo concentration than uranium oxides samples, of 455.2 ± 25.8 µg/g and 1372.0 ± 70.9 µg/g respectively. These Mo concentrations are different from certified values[24] by 8.6 % and 15.4 % respectively, which could be explained by different sample treatments prior to our analysis. While we directly acid-digested our sample aliquots, samples were dried at 110°C

or calcined at 900 °C before weighing and determination of the certified values[24]. Difference between the two protocols can be perfectly explained by the loss of the water molecules constitutive of diuranates, during heating (e.g. sodium diuranate = $Na_2U_2O_7.6H_2O$). The two diuranate samples show a large mass-dependent Mo isotope fractionation with δ^{98}Mo values of -2.84 ± 0.03 ‰ and -1.82 ± 0.03 ‰ (2 SE) respectively.

In the nuclear fuel cycle, uranium ore concentrates are produced from uranium ores after a series of processes aiming at purifying and concentrating uranium until reaching a grade of 85 wt.%. Uranium is first leached almost quantitatively by acid (H_2SO_4) or alkaline (Na_2CO_3) solutions. Resin ion-exchange chromatography and/or solvent extraction, followed by uranium oxide precipitation, are used to partially remove other contaminants, such as Mo, As, Fe, Zr, etc. After drying, uranium ore concentrates are produced in the form of diuranate (such as $Na_2U_2O_7.6H_2O$ or $MgU_2O_7.6H_2O$) at this stage. Uranium ore concentrates in the form of U_3O_8 are produced after calcination of the former at temperatures ranging from 600 to 900°C. Mass-dependent Mo isotope fractionations were already reported during resin ion-exchange chromatography[3, 5] when Mo is partially eluted and this could also occur during the nuclear fuel cycle. Kinetic and/or equilibrium fractionations could occur also during the removal of Mo at all steps of the uranium concentration and purification processes, leading to an enrichment of the lighter Mo isotopes in uranium ore concentrates. Alternatively, addition of an unknown solution of Mo for the fabrication of the two U_3O_8 reference materials, Bolet and Chanterelle, could explain their much higher δ^{98}Mo values, overwhelming any Mo isotope signature that was originally present[24]. In contrast, the two diuranate reference materials, Grenat and Calcedoine, were not spiked with Mo solutions and reflect isotope ratios inherited from the ores and the industrial processes[24]. Altogether, the existence of Mo isotope fractionation is promising for applications in nuclear forensics but would require more in-depth investigations to identify the source of fractionation.

7. Conclusions

We have developed a new method for the separation of molybdenum from geological and uranium-rich samples, with a three-stage ion-exchange chromatography. A high degree of purification from matrix and isobarically interfering elements was obtained, with Mo yields ranging from 42 to 80 % (mean value: 60 ± 17 %, 2 SD). Mo isotopic compositions were measured on a Neptune Plus MC-ICP-MS equipped with Jet cones, and this method allowed the measurements of solutions with Mo concentration close to 30 ng/ml. The sensitivity achieved with our setup is ~1200-1600 V/ppm (aspiration rate ~150 µl/min), which is at least a factor of 10 better than in most previous reports. The level of isobaric interferences was controlled by stringent purification of the samples combined with careful monitoring and limitation of interferences produced in the plasma source itself. Chemical and instrumental mass fractionations were both efficiently corrected using the double spike method. The large range of δ^{98}Mo values in some uranium ore concentrates standards suggest that Mo

isotopes have a strong potential as a tracer for the origin of uranium ores and/or uranium purification processes in the nuclear fuel cycle.

Acknowledgements

We thank the two anonymous referees for their insightful comments. Philippe Telouk is thanked for technical support on the Neptune Plus.

References

1. J. R. De Laeter, J. K. Böhlke, P. De Bièvre, H. Hidaka, H. S. Peiser, K. J. R. Rosman and P. D. P. Taylor, *Pure and Applied chemistry*, 2003, 75, 683-800.
2. A. J. Pietruszka, R. J. Walker and P. A. Candela, *Chemical Geology*, 2006, 225, 121-136.
3. A. D. Anbar, K. A. Knab and J. Barling, *Analytical Chemistry*, 2001, 73, 1425-1431.
4. D. Malinovsky, I. Rodushkin, D. C. Baxter, J. Ingri and B. Öhlander, *International Journal of Mass Spectrometry*, 2005, 245, 94-107.
5. C. Siebert, T. F. Nägler and J. D. Kramers, *Geochemistry Geophysics Geosystems*, 2001, 2, 1-16.
6. C. Burkhardt, T. Kleine, F. Oberli, A. Pack, B. Bourdon and R. Wieler, *Earth and Planetary Science Letters*, 2011, 312, 390-400.
7. J. Barling, G. L. Arnold and A. D. Anbar, *Earth and Planetary Science Letters*, 2001, 193, 447-457.
8. Y. Duan, A. D. Anbar, G. L. Arnold, T. W. Lyons, G. W. Gordon and B. Kendall, *Geochimica et Cosmochimica Acta*, 2010, 74, 6655-6668.
9. C. R. Pearce, A. S. Cohen and I. J. Parkinson, *Geostandards and Geoanalytical Research*, 2009, 33, 219-229.
10. C. Burkhardt, T. Kleine, F. Oberli, A. Pack, B. Bourdon and R. Wieler, *Earth and Planetary Science Letters*, 2011, 312, 390-400.
11. T. Fujii, F. Moynier, P. Telouk and F. Albarède, *Astrophysics Journal*, 2006, 647, 1506-1516.
12. J.L. Morford and S. Emerson, *Geochimica et Cosmochimica Acta*, 1999, 63, 1735-1750.
13. G. Chaillou, P. Anschutz, G. Lavaux, J. Schäfer and G. Blanc, *Marine Chemistry*, 2002, 80, 41-59.
14. B. Sundby, P. Martinez and C. Gobeil, *Geochimica et Cosmochimica Acta*, 2004, 68, 2485-2493.
15. Y. Zheng, R. F. Anderson, A. van Green and J. Kuwabara, *Geochimica et Cosmochimica Acta*, 2000, 64, 4165-4178.
16. W. E. Dean, J. V. Gardner and D. Z. Piper, *Geochimica et Cosmochimica Acta*, 1997, 61, 4507-4518.
17. J. M. Adelson, G. R. Helz and C. V. Miller, *Geochimica et Cosmochimica Acta*, 2001, 65, 237-252.
18. N. Tribovillard, T. J. Algeo, F. Baudin and A. Riboulleau, *Chemical Geology*, 2012, 324-325, 46-58.
19. UDEPO, World Distribution of Uranium Deposits, https://infcis.iaea.org.
20. W. E. Thompson, W. V. Swarenski, D. L. Warner, G. E. Rouse, O. F. Carrington and R. Z. Pyrih, *Ground-Water Elements of In Situ Leach Mining of Uranium*, U.S. Nuclear Regulatory Commission Tampa, Florida, 1978.
21. E. Keegan, S. Richter, I. Kelly, H. Wong, P. Gadd, H. Kuehn and A. Alonso-Munoz, *Applied Geochemistry*, 2008, 23, 765-777.

22. C. K. Gupta, *Extractive Metallurgy of Molybdenum*, CRC Press, USA, 1992.
23. I. Wagani, PhD thesis, Université Paris Sud-XI, 2007.
24. CETAMA, Reference materials catalogue, http://www-cetama.cea.fr/home/.
25. IAEA, *Uranium extraction technology*, IAEA, 1993.
26. A. Le-Boudec, Ph.D. thesis, Ecole Normale Supérieure de Lyon, 2013.
27. F. W. E. Strelow and C. J. C. Bothma, *Analytical Chemistry*, 1967, 39, 595-599.
28. N. Dauphas, L. Reisberg and B. Marty, *Analytical Chemistry*, 2001, 73, 2613-2616.
29. L. Qi and A. Masuda, *International Journal of Mass Spectrometry and Ion Physics*, 1994, 130, 65-72.
30. H. Wen, J. Carignan, C. Cloquet, X. Zhu and Y. Zhang, *Journal of Analytical Atomic Spectrometry*, 2010, 25, 716-721.
31. N. D. Greber, C. Siebert, T. F. Nägler and T. Pettke, *Geostandards and Geoanalytical Research*, 2012, 36, 291-300.
32. T. Goldberg, G. Gordon, G. Izon, C. Archer, C. R. Pearce, J. McManus, A. D. Anbar and M. Rehkamper, *Journal of Analytical Atomic Spectrometry*, 2013, 28, 724-735.
33. J. Li, X.-R. Liang, L.-F. Zhong, X.-C. Wang, Z.-Y. Ren, S.-L. Sun, Z.-F. Zhang and J.-F. Xu, *Geostandards and Geoanalytical Research*, 2014, 1-10.
34. J. Mizera and Z. Randa, *Journal of Radioanalytical and Nuclear Chemistry*, 2010, 284, 157-163.
35. J. Carignan, P. Hild, G. Mevelle, J. Morel and D. Yeghicheyan, *Geostandards Newsletter*, 2001, 25, 187-198.
36. S. Terashima, *Geostandards Newsletter*, 1997, 21, 93-96.
37. W. A. Russel, D. A. Papanastassiou and T. A. Tombrello, *Geochimica et Cosmochimica Acta*, 1978, 42, 1075-1090.
38. S. J. G. Galer, *Chemical Geology*, 1999, 157, 255-274.
39. M. H. Dodson, *Journal of Scientific Instrument*, 1963, 40, 289-295.
40. J. F. Rudge, B. C. Reynolds and B. Bourdon, *Chemical Geology*, 2009, 265, 420-431.
41. J. Korkish, *Handbook of Ion-Exchange Resins : their Application to Inorganic Analytical Chemistry*, New York, 1989.
42. A. Kronenberg, P. K. Mohapatra, J. V. Kratz, G. Pfrepper and F. Pfrepper, *Radiochimica Acta*, 2004, 92, 395-403.
43. C. Burkhardt, R. C. Hin, T. Kleine and B. Bourdon, *Earth and Planetary Science Letters*, 2014, 391, 201-211.
44. L. Xu, B. Lehmann, J. Mao, T. F. Nägler, N. Neubert, M. E. Böttcher and P. Escher, *Chemical Geology*, 2012, 318, 45-59.
45. A. D. Herrmann, B. Kendall, T. J. Algeo, G. W. Gordon, L. E. Wasylenki and A. D. Anbar, *Chemical Geology*, 2012, 324, 87-98.
46. C. Siebert, T. F. Nägler, F. Von Blanckenburg and J. D. Kramers, *Earth and Planetary Science Letters*, 2003, 211, 159-171.
47. C. Burkhardt, T. Kleine, N. Dauphas and R. Wieler, *Earth and Planetary Science Letters*, 2012, 357-358, 298-307.
48. A. R. Voegelin, T. F. Nägler, E. Samankassou and I. M. Villa, *Chemical Geology*, 2009, 265, 488-498.